



**HAL**  
open science

## Structure and white LED properties of Ce-doped YAG-Al<sub>2</sub>O<sub>3</sub> eutectics grown by the micro-pulling-down method

Qingsong Song, Xiaodong Xu, Jian Liu, Xiangshai Bu, Dongzhen Li, Peng  
Liu, Yinzhen Wang, Jun (jim) Xu, Kheirredine Lebbou

► **To cite this version:**

Qingsong Song, Xiaodong Xu, Jian Liu, Xiangshai Bu, Dongzhen Li, et al.. Structure and white LED properties of Ce-doped YAG-Al<sub>2</sub>O<sub>3</sub> eutectics grown by the micro-pulling-down method. *CrystEngComm*, 2019, 21 (31), pp.4545-4550. 10.1039/c9ce00703b . hal-02367594

**HAL Id: hal-02367594**

**<https://univ-lyon1.hal.science/hal-02367594>**

Submitted on 4 Feb 2021

**HAL** is a multi-disciplinary open access archive for the deposit and dissemination of scientific research documents, whether they are published or not. The documents may come from teaching and research institutions in France or abroad, or from public or private research centers.

L'archive ouverte pluridisciplinaire **HAL**, est destinée au dépôt et à la diffusion de documents scientifiques de niveau recherche, publiés ou non, émanant des établissements d'enseignement et de recherche français ou étrangers, des laboratoires publics ou privés.

# Structure and White LED Properties of Ce-doped YAG-Al<sub>2</sub>O<sub>3</sub> Eutectics Grown by the Micro-Pulling-Down Method

QINGSONG SONG,<sup>1</sup> XIAODONG XU,<sup>1,\*</sup> JIAN LIU,<sup>1</sup> XIANGSHAI BU,<sup>1</sup> DONGZHEN LI,<sup>1</sup> PENG LIU,<sup>1</sup> YINZHEN WANG,<sup>2</sup> JUN XU,<sup>3</sup> AND KHEIRREDDINE LEBBOU<sup>4</sup>

<sup>1</sup> Jiangsu Key Laboratory of Advanced Laser Materials and Devices, School of Physics and Electronic Engineering, Jiangsu Normal University, Xuzhou 221116, China

<sup>2</sup> School of Physics and Telecommunication Engineering, South China Normal University, Guangzhou, 510006, China

<sup>3</sup> School of Physics Science and Engineering, Institute for Advanced Study, Tongji University, Shanghai 200092, China

<sup>4</sup> Institut Lumière Matière, UMR5306 Université Lyon1-CNRS, Université de Lyon, Lyon 69622, Villeurbanne Cedex, France

\* xdxu79@mail.sic.ac.cn

**Abstract:** A series of Ce-doped YAG-Al<sub>2</sub>O<sub>3</sub> eutectics were grown by the micro-pulling-down ( $\mu$ -PD) method, for the purpose of high power white light emitting diodes. The eutectic structure was investigated. A calibrated integrating sphere spectrometer setup was used to measure the white LED properties of eutectic samples. The CIE color coordinates can be regulated easily by altering the Ce<sup>3+</sup> doping concentration and sample thickness of the Ce:YAG-Al<sub>2</sub>O<sub>3</sub> eutectics. A 1 W white LED device based on Ce:YAG-Al<sub>2</sub>O<sub>3</sub> eutectics under rated current of 350 mA emitted a bright white light with a CIE coordinate of (0.319, 0.334), a luminous efficiency of 83.0 lm/W and a Duv value of 0.003. The results showed that Ce:YAG-Al<sub>2</sub>O<sub>3</sub> eutectics have better luminous properties than commercial powder phosphors at high current density.

---

## References and links

- [1] Z. Xia, A. Meijerink, "Ce<sup>3+</sup>-doped garnet phosphors: composition modification, luminescence properties and applications," *Chem. Soc. Rev.* **46**(1), 275-299 (2017).
- [2] C. Basu, M. Meinhardt-Wollweber, and B. Roth, "Lighting with laser diodes," *Adv. Opt. Techn.* **2**(4), 313-321 (2013).
- [3] K. Li, Y. Shi, F. Jia, C. Price, Y. Gong, J. Huang, N. Copner, H. Cao, L. Yang, S. Chen, H. Chen, and J. Li, "Low extendue yellow-green solid-state light generation by laser-pumped LuAG:Ce ceramic," *IEEE Photonics Technol. Lett.* **30**(10), 939-942 (2018).
- [4] B.-J. Shih, S.-C. Chiou, Y.-H. Hsieh, C.-C. Sun, T.-H. Yang, S.-Y. Chen, and T.-Y. Chung, "Study of temperature distributions in pc-WLEDs with different phosphor packages," *Opt. Express* **23**(26) 33861-33869 (2015).
- [5] I. U. Perera, N. Narendran, "Analysis of a remote phosphor layer heat sink to reduce phosphor operating temperature," *Int. J. Heat Mass Transfer* **117**, 211-222 (2018).
- [6] A. Krasnoshchoka, A. Thorseth, C. Dam-Hansen, D. D. Corell, P. M. Petersen and O. B. Jensen, "Investigation of saturation effects in ceramic phosphors for laser lighting," *Materials* **10**(12), 1407 (2017).
- [7] Y. Yang, S. Zhuang, B. Kai, "High brightness laser-driven white emitter for extendue-limited applications," *Appl. Opt.* **56**(30), 8321-8325 (2017).
- [8] Y. H. Kim, N. S. M. Viswanath, S. Unithrattil, H. J. Kim, and W. B. Im, "Review-phosphor plates for high-power LED applications: Challenges and opportunities toward perfect lighting," *ECS J. Solid State Sci. Technol.* **7**(1), R3134-R3147 (2018).
- [9] P. Zheng, S. Li, L. Wang, T. Zhou, S. You, T. Takeda, N. Hirosaki, and R.-J. Xie, "A unique color converter architecture enabling phosphor-in-glass (PiG) films suitable for high-power and high-luminance laser-driven white lighting," *ACS Appl. Mat. Interfaces* **10**(17), 14930-14940 (2018).
- [10] Y. Peng, Y. Mou, H. Wang, Y. Zhuo, H. Li, M. Chen, and X. Luo, "Stable and efficient all-inorganic color converter based on phosphor in tellurite glass for next-generation laser-excited white lighting," *J. Eur. Ceram. Soc.* **38**(16), 5525-5532 (2018).
- [11] C. Ma, Y. Cao, X. Shen, Z. Wen, R. Ma, J. Long, and X. Yuan, "High reliable and chromaticity-tunable flip-

- chip w-LEDs with Ce:YAG glass-ceramics phosphor for long-lifetime automotive headlights applications,” *Opt. Mater.* **69**, 105-114 (2017).
- [12] E. G. Villora, K. Shimamura, D. Inomata, and K. Iizuka, “Single-crystal phosphors for high-brightness white lighting,” *Proc. SPIE* **9768**, 976805 (2016).
- [13] G. Liu, Z. Zhou, Y. Shi, Q. Liu, J. Wan, and Y. Pan, “Ce:YAG transparent ceramics for applications of high power LEDs: Thickness effects and high temperature performance,” *Mater. Lett.* **139**, 480-482 (2015).
- [14] S. Hu, C. Lu, G. Zhou, X. Liu, X. Qin, G. Liu, S. Wang, and Z. Xu, “Transparent YAG:Ce ceramics for WLEDs with high CRI: Ce<sup>3+</sup>, concentration and sample thickness effects,” *Ceram. Int.* **42**(6), 6935-6941 (2016).
- [15] J. Xu, B. Hu, Z. Liu, Y. Gong, B. Hu, J. Wang, H. Li, X. Wang, and B. Du, “Design of laser-driven SiO<sub>2</sub>-YAG:Ce composite thick film: Facile synthesis, robust thermal performance, and application in solid-state laser lighting,” *Opt. Mater.* **75**, 508-512 (2018).
- [16] Q. Sai, Z. Zhao, C. Xia, X. Xu, F. Wu, J. D, and L. Wang, “Ce-doped Al<sub>2</sub>O<sub>3</sub>-YAG eutectic and its application for white LEDs,” *Opt. Mater.* **35**(12), 2155-2159 (2013).
- [17] Y. Liu, M. Zhang, Y. Nie, J. Zhang, and J. Wang, “Growth of YAG:Ce<sup>3+</sup>-Al<sub>2</sub>O<sub>3</sub> eutectic ceramic by HDS method and its application for white LEDs,” *J. Eur. Ceram. Soc.* **37**(15), 4931-4937 (2017).
- [18] Q. Sai, C. Xia, “Tunable colorimetric performance of Al<sub>2</sub>O<sub>3</sub>-YAG:Ce<sup>3+</sup>, eutectic crystal by Ce<sup>3+</sup>, concentration,” *J. Lumin.* **186**, 68-71 (2017).
- [19] S. Li, Q. Zhu, D. Tang, X. Liu, G. Ouyang, L. Cao, N. Hirotsaki, T. Nishimura, Z. Huang, and R.-J. Xie, “Al<sub>2</sub>O<sub>3</sub>-YAG:Ce composite phosphor ceramic: a thermally robust and efficient color converter for solid state laser lighting,” *J. Mater. Chem. C* **4**(37), 8648—8654 (2016).
- [20] R. Simura, T. Taniuchi, K. Sugiyama, and T. Fukuda, “Textural and optical properties of Ce-doped YAG/Al<sub>2</sub>O<sub>3</sub> melt growth composite grown by micro-pulling-down method,” *High Temp. Mater. Proc.* **37**(2), 127-131 (2018).
- [21] Y. Tang, S. Zhou, C. Chen, X. Yi, Y. Feng, H. Lin, and S. Zhang, “Composite phase ceramic phosphor of Al<sub>2</sub>O<sub>3</sub>-Ce:YAG for high efficiency light emitting,” *Opt. Express* **23**(14), 17923-17928 (2015).
- [22] Y. H. Song, E. K. Ji, B. W. Jeong, M. K. Jung, E. Y. Kim, C. W. Lee, and D. H. Yoon, “Design of laser-driven high-efficiency Al<sub>2</sub>O<sub>3</sub>/YAG:Ce<sup>3+</sup>, ceramic converter for automotive lighting: Fabrication, luminous emittance, and tunable color space,” *Dyes Pigm.* **139**, 688-692 (2017).
- [23] S. Hu, Y. Zhang, Z. Wang, G. Zhou, Z. Xue, H. Zhang, and S. Wang, “Phase composition, microstructure and luminescent property evolutions in “light-scattering enhanced” Al<sub>2</sub>O<sub>3</sub>-Y<sub>3</sub>Al<sub>5</sub>O<sub>12</sub>:Ce<sup>3+</sup>, ceramic phosphors,” *J. Eur. Ceram. Soc.* **38**, 3268–3278 (2018).
- [24] K. Lebbou, “Single crystals fiber technology design. Where we are today?,” *Opt. Mater.* **63**, 13-18 (2017).
- [25] A. Djebli, F. Boudjada, K. Pauwels, V. Kononets, G. Patton, A. Benaglia, M. Lucchini, F. Moretti, O. Sidletskiy, C. Dujardin, P. Lecoq, E. Auffray, and K. Lebbou, “Growth and characterization of Ce-doped YAG and LuAG fibers,” *Opt. Mater.* **65**, 66-68(2017).
- [26] F. H. Chung, “Quantitative interpretation of X-ray diffraction patterns of mixtures. III. Simultaneous determination of a set of reference intensities,” *J. Appl. Cryst.* **8**(1),17-19 (1975).
- [27] R. Simura, A. Yoshikawa, and S. Uda, “The radial distribution of dopant (Cr, Nd, Yb, or Ce) in yttrium aluminum garnet (Y<sub>3</sub>Al<sub>5</sub>O<sub>12</sub>) single crystals grown by the micro-pulling-down method,” *J. Cryst. Growth* **311**(23), 4763-4769 (2009).
- [28] X. Xu, K. Lebbou, F. Moretti, K. Pauwels, P. Lecoq, E. Auffray, and C. Dujardin, “Ce-doped LuAG single-crystal fibers grown from the melt for high-energy physics,” *Acta Mater.* **67**(15), 232-238 (2014).
- [29] A. Yoshikawa, B. M. Epelbaum, K. Hasegaw, S. D. Durbin, and T. Fukuda, “Microstructures in oxide eutectic fibers grown by a modified micro-pulling-down method,” *Cryst. Growth* **205**(3), 305-316 (1999).
- [30] Y. Zhou, J. Lin, M. Yu, S. Wang, and H. Zhang, “Synthesis-dependent luminescence properties of Y<sub>3</sub>Al<sub>5</sub>O<sub>12</sub>:Re<sup>3+</sup> (Re=Ce, Sm, Tb) phosphors,” *Mater. Lett.* **56**(5), 628-636 (2002).
- [31] D. Haranath, H. Chander, P. Sharma, and S. Singh, “Enhanced luminescence of Y<sub>3</sub>Al<sub>5</sub>O<sub>12</sub>:Ce<sup>3+</sup> nanophosphor for white light-emitting diodes,” *Appl. Phys. Lett.* **89**, 173118 (2006).
- [32] A. P. Piquettea, M. E. Hannaha, and K. C. Mishra, “An investigation of self-absorption and corresponding spectral shift in phosphors,” *ECS Trans.* **41**(37), 1-9 (2012).
- [33] J. Sathian, J. D. Breeze, B. Richards, N. M. Alford, and M. Oxborrow, “Solid-state source of intense yellow light based on a Ce:YAG luminescent concentrator,” *Opt. Express* **25**(12), 13714-13727 (2017).
- [34] H. V. Demir, S. N. Nizamoglu, T. Erdem, E. Mutlugun, N. Gaponik, and A. Eychmüller, “Quantum dot integrated LEDs using photonic and excitonic color conversion,” *Nano Today* **6**(6), 632-647 (2011).
- [35] ANSI, “American national standard for electric lamps—Specifications for the chromaticity of solid state lighting (SSL) products,” ANSI C78.377–2015 (American National Standard Institute, 2015).

## 1. Introduction

Solid-state lighting (SSL) changes the way we light the world. White light-emitting diodes (WLEDs) are now the preferred light source for SSL. The WLED lighting system is a mature technology, which normally combines visible radiation from a blue GaN chip with the emission from Ce:Y<sub>3</sub>Al<sub>5</sub>O<sub>12</sub> (Ce:YAG) yellow emitting phosphor powder dispersed in resin or silica gel [1]. However, in the phosphor-converted WLED system, the heat generated from the LED chip and the wavelength-converting phosphor can't be efficiently discharged on account of the poor thermal conductivity of the resin, which increases LED junction temperature. The performance of WLED systems depends mainly on temperature factors, which causes luminous decay and color shifting in the WLED because of the thermal quenching properties of the phosphors [2].

With the development of GaN-based blue LEDs and laser diodes (LDs), the high-brightness solid state lighting has attracted a wide range of interests in both academy and industry and requires higher temperature adaptability for lighting equipment [3]. In the past few years, many methods have been utilized to reduce phosphor operating temperature in phosphor-converted WLED, such as changing LED chip package structure [4,5] and improving the thermal conductivity phosphors materials [6-8]. Phosphor plates, including phosphor-in-glasses [9,10], glass phosphors [11], single-crystal phosphors [12] and ceramic phosphors [13-15], instead of phosphor powder dispersed in resin/silica gel were widely studied. Among them, Ce:YAG transparent ceramics and Ce:YAG-Al<sub>2</sub>O<sub>3</sub> eutectic ceramics exhibit good fluorescence performance and temperature stability [16-18]. Compared with Ce:YAG ceramics, the Ce:YAG-Al<sub>2</sub>O<sub>3</sub> eutectics ceramic shows a higher thermal conductivity of 18.5 W m<sup>-1</sup> K<sup>-1</sup>. At 200°C, its fluorescence intensity only reduces 8%, which is better than 10% of YAG:Ce ceramics [19]. Rayko Simura et al. first attempted to produce Ce:YAG-Al<sub>2</sub>O<sub>3</sub> eutectics by the  $\mu$ -PD method and the measured fluorescence intensity of the sample at 200°C decreased no more than 8% [20], which was comparable with that of Ce:YAG-Al<sub>2</sub>O<sub>3</sub> eutectic ceramics.

Although researchers have done a lot of work on Ce:YAG-Al<sub>2</sub>O<sub>3</sub> eutectics [21-23], data on LED properties of the eutectics with different Ce<sup>3+</sup> concentration is still insufficient. In order to obtain the data, the  $\mu$ -PD method is a good choice. The method is an economical and quick crystal growth method from the melt, and allows the growth of fiber-like samples with diameters in the range from 0.15 mm to 5 mm at a variable pulling rate (0.01-10 mm/min) [24, 25].

In this paper, a series of Ce-doped YAG-Al<sub>2</sub>O<sub>3</sub> eutectics have been grown by the  $\mu$ -PD Method. Structure of the eutectics was examined by X-ray diffraction (XRD) and scanning electron microscopy (SEM). The effect of Ce concentration and slice thickness on the properties of the eutectics was studied. The spectral power distribution (SPD), CIE chromaticity coordinates, correlated color temperature (CCT) and distance between source and blackbody curve (D<sub>uv</sub>) were discussed.

## 2. Eutectic growth and structure

The Ce:YAG-Al<sub>2</sub>O<sub>3</sub> eutectics were grown using the  $\mu$ -PD method. Raw materials of Y<sub>2</sub>O<sub>3</sub> (99.999%), Al<sub>2</sub>O<sub>3</sub> (99.999%), and CeO<sub>2</sub> (99.99%) were weighted according to the formula (Y<sub>1-x</sub>Ce<sub>x</sub>)<sub>3</sub>Al<sub>5</sub>O<sub>12</sub>-Al<sub>2</sub>O<sub>3</sub> (x=0.05%, 0.15%, 0.25%, 0.35% 0.50%, 0.75%, the mole ratio of Al<sub>2</sub>O<sub>3</sub>/Y<sub>2</sub>O<sub>3</sub> is 81/19). The starting materials were mixed thoroughly in an agate mortar and pre-sintered in a muffle furnace for 10 h at 1200°C. Then the polycrystalline materials were loaded into an iridium crucible for crystal growth. The Ce:YAG-Al<sub>2</sub>O<sub>3</sub> eutectics were pulled through the capillary channel at the bottom of the crucible. The capillary outer diameter was 2 mm. A <111> orientation YAG seed was used as the seed and the pulling rate was 0.5 mm/min. The solid-liquid interface and the growing eutectics were observed using a CCD camera. In order to avoid oxidation of the Ir crucible and after heater, the flowing Ar atmosphere was used during the solidification process. The obtained Ce:YAG-Al<sub>2</sub>O<sub>3</sub> eutectic rods with different Ce concentration are shown in Fig. 1(a). The rods are bright yellow and have a diameter of about 2.0 mm. Fig. 1(b) shows a polished eutectic slice of 0.35 at.%

Ce:YAG-Al<sub>2</sub>O<sub>3</sub> eutectic with a thickness of 0.3 mm. It can be seen that the slice was translucent.

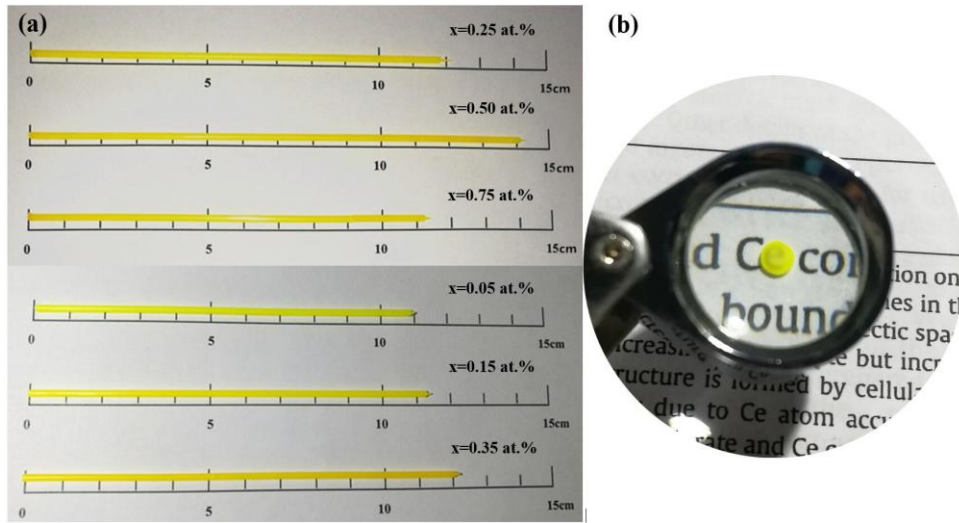


Fig. 1 Photograph of the as-grown Ce:YAG-Al<sub>2</sub>O<sub>3</sub> eutectics (a) rods and (b) slice

The crystalline phases of the as-grown eutectics were examined with x-ray powder diffraction (XRD, Bruker-D2, Germany). The XRD patterns of Ce:YAG-Al<sub>2</sub>O<sub>3</sub> eutectics are shown in Fig. 2. The diffraction peaks reveal that only the YAG and Al<sub>2</sub>O<sub>3</sub> phases exist in the eutectic system and no impurity phases were observed. From the adiabatic principle of X-ray diffraction analysis of mixtures [26], the weight ratio of the two phases can be roughly calculated by the formula:

$$I_Y/I_C = K \cdot w_Y/w_C \quad (1)$$

Where  $I_Y$  and  $I_C$  are the X-ray strongest intensity of YAG and corundum  $c$ . The value of reference intensity  $K$  is 4.38, which can be found from PDF#88-2048.  $w_Y$  and  $w_C$  is weight percentage of component YAG and corundum  $c$ . Assumed that the Al<sub>2</sub>O<sub>3</sub> is corundum phase, the weight ratio of YAG and Al<sub>2</sub>O<sub>3</sub> was calculated to be 1.42, which is very close to the ratio of the initial material of 1.43.

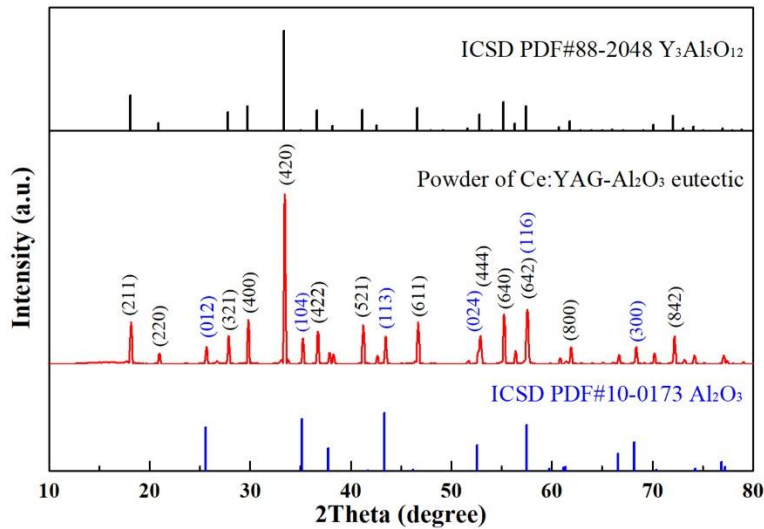


Fig. 2 The XRD pattern of Ce:YAG-Al<sub>2</sub>O<sub>3</sub> eutectic powder

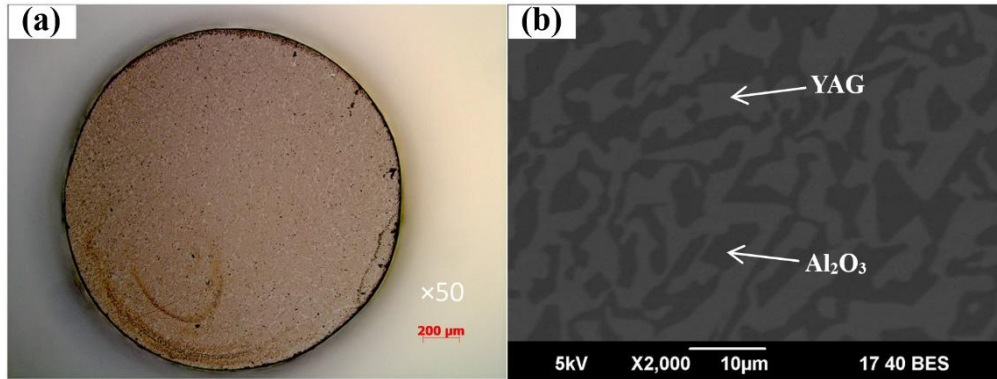


Fig. 3(a) Optical microscopy image and (b) the backscattered electron image of Ce:YAG- $\text{Al}_2\text{O}_3$  eutectic

The morphology of Ce:YAG- $\text{Al}_2\text{O}_3$  eutectic was analyzed with a Zeiss optical microscope and a scanning electron microscope (SEM, JSM6390, JEOL, Kariya, Japan). Fig. 3a shows a transverse cross-section of a Ce:YAG- $\text{Al}_2\text{O}_3$  eutectic grown from starting melt containing 0.75 at.% Ce. Different from the  $\text{Ce}^{3+}$  concentration distribution in YAG and LuAG crystals [27, 28], the  $\text{Ce}^{3+}$  concentration distribution is uniform in the eutectics and no visible concentration gradient can be observed. The backscattered electron image of the eutectic microstructure is shown in Fig. 3b. As observed by X-ray powder diffraction, only two phases exist. The dark region corresponds to the  $\alpha\text{-Al}_2\text{O}_3$  phase and the grey region corresponds to the YAG phase. The microstructure resembles an irregularly twisted lamellar structure, commonly referred as “Chinese Script” microstructure [29]. The boundaries between the phases were clearly marked. There is no morphology or microstructure fluctuation along the grown fibers. The morphologies analysis in the beginning, middle and the end of the fiber is the same.

### 3. Spectral properties

The samples were cut from the as-grown eutectics and two surfaces perpendicular to the grow direction were polished for spectral measurements. A fluorescence spectrometer (FLS920, Edinburgh Instruments, Edinburgh) was adopted to measure the excitation and emission spectra of Ce:YAG- $\text{Al}_2\text{O}_3$  eutectic. Fig. 4 shows the photoluminescence (PL) and photoluminescence excitation (PLE) spectra of 0.15 at.% Ce:YAG- $\text{Al}_2\text{O}_3$  eutectic. The PLE spectrum shows two bands centered at 343 and 456 nm originating from the  $5d \rightarrow 4f$  transition of  $\text{Ce}^{3+}$ . The 456 nm excitation peak has a full width at half maximum (FWHM) of 76.5 nm, which matches well with blue LED chips of different wavelengths. The eutectic exhibits a typical  $\text{Ce}^{3+}$ :  $5d \rightarrow 4f$  broadband emission centered at 542 nm under 450 nm excitation, which corresponds to doublet sub-emissions from  $5d_1 \rightarrow {}^2F_{7/2}$  and  $5d_1 \rightarrow {}^2F_{5/2}$  transitions of  $\text{Ce}^{3+}$  ions.

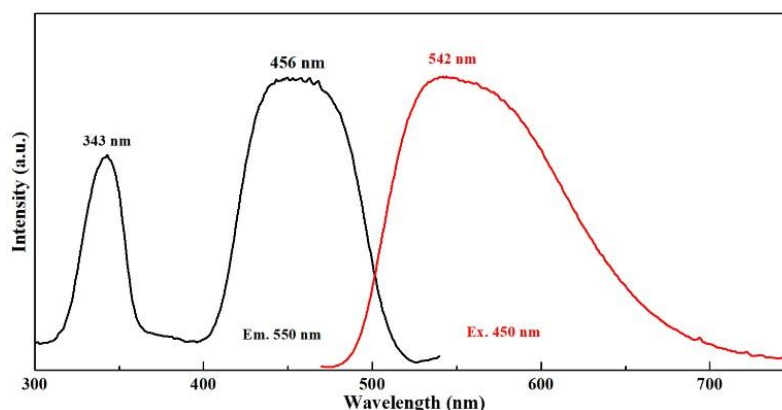


Fig. 4 PL and PLE spectra of 0.15 at. % Ce:YAG-Al<sub>2</sub>O<sub>3</sub> eutectic.

A blue LED chip was used to test the performance of eutectics. The rated current, power, emission wavelength and size of the blue LED chip were 350 mA, 1 W, 450.2 nm and  $0.74 \times 0.74 \text{ mm}^2$ , respectively. To measure the SPD, luminous efficacy (LE), color coordinates, CCT, color rendering index (Ra) and  $D_{uv}$  of the eutectic samples with different Ce content and thickness, a setup consisting of an integrating sphere from Hopoo and a spectrometer from Everfine (CAS200) was used.

Fig. 5a presents the absolute SPDs of Ce:YAG-Al<sub>2</sub>O<sub>3</sub> eutectics prepared using various Ce<sup>3+</sup> doping concentration. The absolute SPD is the sum of the eutectic emissions and the non-absorbed blue light. All eutectic samples show a broad emission peak in the range of 485-700 nm. With increasing the doping concentration from 0.05 at.% to 0.75 at.%, a red shift of about 19 nm was observed for the position of the emission band maximum as shown in the inset of Fig. 5a, which was attributed to the intensified crystal field around Ce<sup>3+</sup> ions [30, 31]. As doping concentration increased, the intensity of blue light penetrating through the eutectic samples was found to decrease for being absorbed by luminescence center directly or through the lattice. However, the intensity of greenish yellow light did not increase monotonously. It increased with doping concentration from 0.05 at.% to 0.35 at.%, because the Ce<sup>3+</sup> ions in the eutectics activate emission. Furthermore, increasing the doping concentration decreased the emission intensity, because of the concentration quenching effect [31]. The absolute SPDs of 0.35 at.% Ce:YAG-Al<sub>2</sub>O<sub>3</sub> eutectic samples with different thickness and the relationship between the wavelength of the emission band maximum and thickness of samples are shown in Fig. 5b. The position of the emission peaks almost kept the same with increasing thickness of eutectic samples. The intensity of greenish yellow light became stronger gradually as the thickness of the eutectics increased from 0.30 to 0.72 mm, and then decreased with further increase of the thickness of the eutectics due to the reabsorption of the emitted light within the eutectics over a long path length along with a reduction in the emission spectra intensity [32,33].

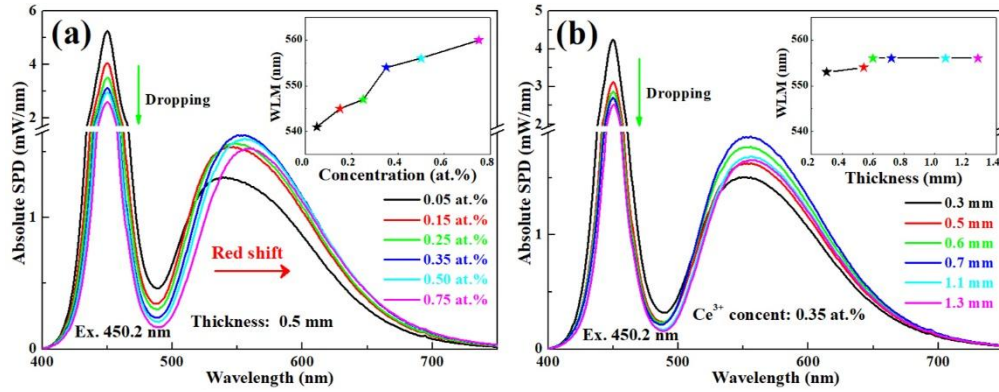


Fig. 5 (a) SPD and the wavelength of emission band maximum (WLM) of Ce:YAG- $\text{Al}_2\text{O}_3$  eutectics with different doping concentration, (b) SPD and the WLM of Ce:YAG- $\text{Al}_2\text{O}_3$  eutectics with different thickness.

Based on the SPDs, chromaticity coordinates for the Ce:YAG- $\text{Al}_2\text{O}_3$  eutectics with different  $\text{Ce}^{3+}$  doping concentration are plotted on the CIE-1931 chromaticity diagram [34], as shown in Fig. 6. With increasing doping concentration in eutectic samples, the color coordinates of eutectics-based LEDs devices shifted from bluish white to yellowish white along with the blackbody locus. To clearly see this change, the photographs of WLEDs with operating current of 350 mA are intuitively displayed in the inset of Fig. 6. The luminous parameters the devices are listed in Table 1, from which one can see that the luminous efficacy increased monotonically with the increase of the doping concentration and reached the optimal value at a doping concentration of 0.35 at.%. However, further increase of the doping concentration resulted in degradation of luminous efficacy. With the increasing  $\text{Ce}^{3+}$  doping concentration in eutectic samples, the CCT decreased from 31180 to 5396 K and the Ra decreased from 77.3 to 65.0. The CCT and  $D_{\text{uv}}$  values of the devices based on Ce:YAG- $\text{Al}_2\text{O}_3$  eutectics with doping concentration of 0.35 at.%, 0.50 at.% and 0.75 at.% were within the range of the standard values in American National Standard Institute (ANSI) C78.377-2015 [35]. Among them, an optimal white LED with a luminous efficacy of 83.0 lm/W, a CCT of 6173 K, a Ra value of 67.3, a  $D_{\text{uv}}$  value of 0.003 and a color coordinate of (0.319, 0.334) was obtained by employing the 0.35 at.% Ce:YAG- $\text{Al}_2\text{O}_3$  eutectic sample.

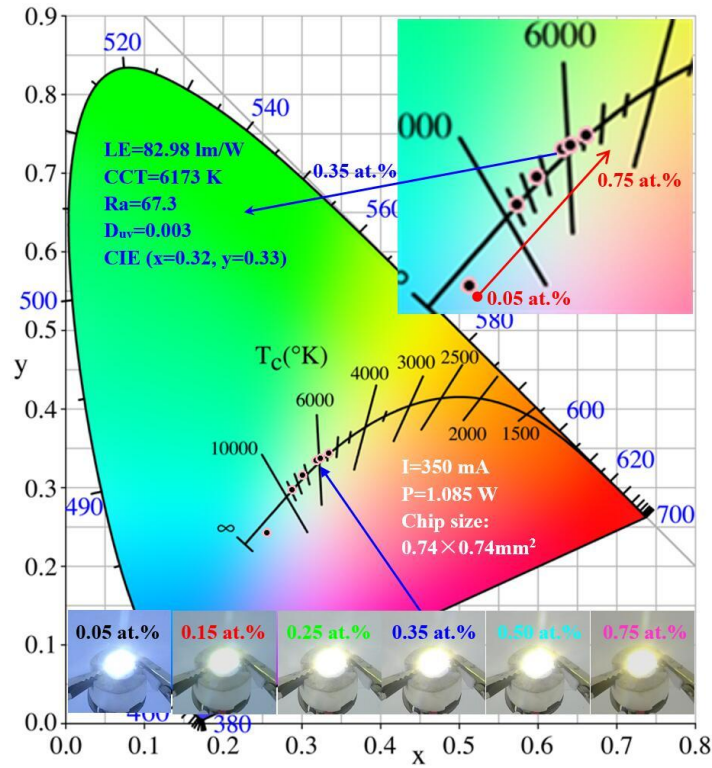


Fig. 6 CIE-1931 (x,y) chromaticity diagram of Ce:YAG-Al<sub>2</sub>O<sub>3</sub> eutectic samples with different doping concentration. The inset presents the luminescent photographs of the eutectics-based LEDs.

Table 1 Luminous parameters of the WLEDs using  $x$ Ce:YAG-Al<sub>2</sub>O<sub>3</sub> ( $x=0.05$ - $0.75$  at.%) eutectics with 0.5 mm thickness.

Ce <sup>3+</sup> content (x, at.%)	CIE color coordinates		LE (lm/W)	CCT (K)	Ra	D <sub>uv</sub>
	x	y				
0.05	0.256	0.243	71.3	31180	77.3	-0.008
0.15	0.288	0.297	81.3	8830	72.2	0.000
0.25	0.301	0.315	81.7	7368	70.2	0.002
0.35	0.319	0.334	83.0	6173	67.3	0.003
0.50	0.324	0.337	80.6	5890	66.6	0.002
0.75	0.335	0.343	75.3	5396	65.0	0.000

Fig. 7 depicts the CIE-1931 chromaticity diagram of 0.35 at.% Ce:YAG-Al<sub>2</sub>O<sub>3</sub> eutectics with different thickness. The color coordinates shifted greatly from bluish white to greenish yellow region with increasing the thickness of eutectics from 0.3 mm to 0.7 mm, and then shifted from greenish yellow to yellowish white. The photographs of WLEDs with operating current of 350 mA are illustrated in the inset of Fig. 7. The luminous parameters the devices are listed in Table 2, from which it can be read that the luminous efficacy increases with increasing sample thickness from 0.3 mm to 0.7 mm and then decreases with increasing sample thickness. The CCT dropped from 9206 to 5238 K and the Ra dropped from 73.1 to

63.1 with the increase of sample thickness. It is noted that the LED based on 0.35 at.% Ce:YAG- $\text{Al}_2\text{O}_3$  eutectic sample with a thickness of 0.7 mm showed a highest luminous efficacy of 93.7 lm/W. However, it also showed a lower Ra value of 63.3 and a larger  $D_{uv}$  value of 0.011, which didn't meet the criteria of lighting requirements. The LED based on the 0.35 at.% Ce:YAG- $\text{Al}_2\text{O}_3$  eutectic sample with a thickness of 0.5 mm showed the optimal luminous parameters, taking into account a compromise of luminous efficacy, CCT, Ra and  $D_{uv}$ .

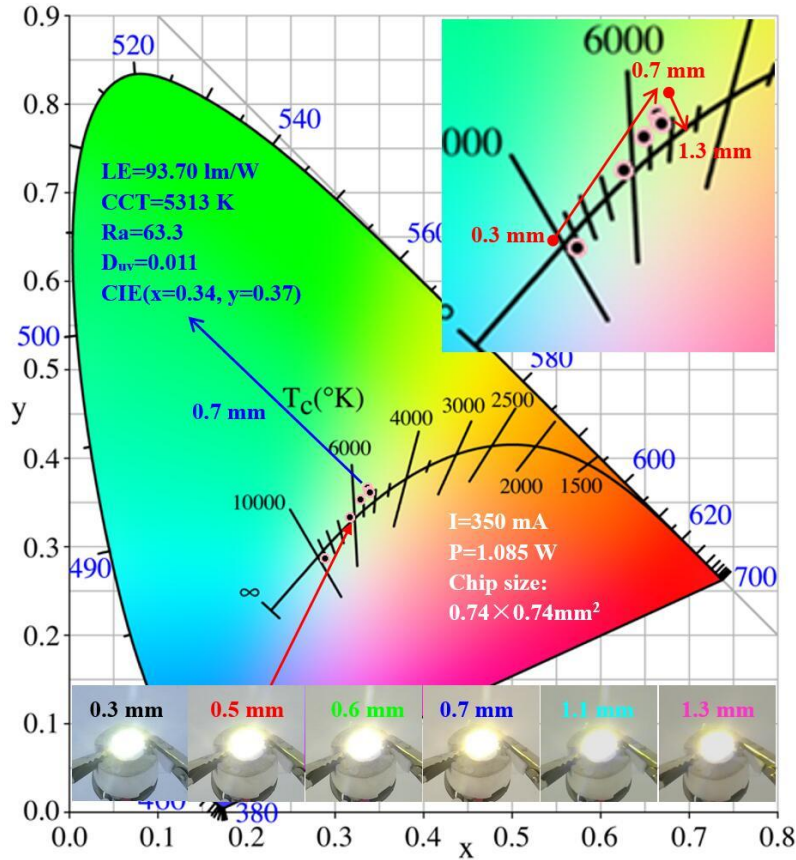


Fig. 7 CIE-1931 (x,y) chromaticity diagram of 0.35 at.% Ce:YAG- $\text{Al}_2\text{O}_3$  eutectic samples with different thickness. The inset presents the luminescent photographs of the eutectics-based LEDs.

Table 2 Luminous parameters of the WLEDs using 0.35 at.% Ce:YAG- $\text{Al}_2\text{O}_3$  eutectics with different thickness.

Thickness (mm)	CIE color coordinates		LE (lm/W)	CCT (K)	Ra	$D_{uv}$
	x	y				
0.3	0.289	0.286	79.2	9206	73.1	-0.006
0.5	0.319	0.334	83.0	6173	67.3	0.003
0.6	0.330	0.354	89.8	5612	65.0	0.008
0.7	0.338	0.367	93.7	5313	63.3	0.011
1.0	0.339	0.363	84.2	5252	63.1	0.008
1.3	0.340	0.361	82.3	5238	63.1	0.007

Fig. 8 presents the current dependence of the CCT (solid lines) and luminous efficacy (dotted lines) of eutectics-based (0.35 at.%, 0.5 mm) LED in comparison to the tendencies of the commercial phosphor-converted white LED based on phosphors and resin. The CCT of both LEDs tend to increase with the increasing value of applied current. The commercial phosphor-converted white LED increases its CCT from 6270 K to 7732 K, while the CCT value of eutectics-based LED was maintained at a relatively small region of 5866–6173 K. With the increase of current density, the luminous efficacy of both LEDs reduces dramatically. The luminous efficacy of eutectics-based LED decreased from 130.7 lm/W to 83.0 lm/W, while commercial package showed almost twice reduction in the same current range: from 173.7 lm/W to 67.4 lm/W. The above results demonstrated that the eutectics-based LED is more promising at higher current density.

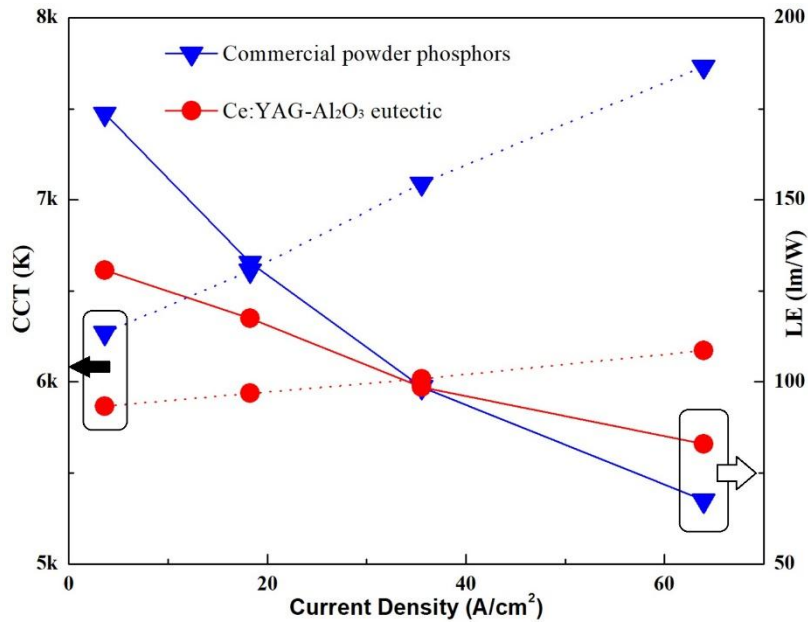


Fig. 8 The CCT (solid lines) and luminous efficacy (dotted lines) of Ce:YAG-Al<sub>2</sub>O<sub>3</sub> eutectics-based LED (triangle) and commercial powder phosphors-based LED (roundness) with the current density of LED.

### 3. Conclusions

In summary, YAG-Al<sub>2</sub>O<sub>3</sub> ceramic eutectics with different Ce<sup>3+</sup> doping concentration were successfully grown by the  $\mu$ -PD method and demonstrated for use in high power white light emitting diodes. The eutectic structure was studied. Among the different Ce<sup>3+</sup> doping concentration and sample thickness, 0.35 at.% Ce:YAG-Al<sub>2</sub>O<sub>3</sub> eutectic with the thickness of 0.5 mm showed the best luminous properties. Under a high rated current of 350 mA, the WLED device with a 1 W blue LED chip showed good luminous performance: a luminous efficiency of 83.0 lm/W, a Duv value of 0.003, a suitable CCT of 6173 K, as well as a CIE coordinate of (0.319, 0.334) near the position of white light. The eutectic showed better luminous properties than commercial powder phosphors at high current density. All the results show that the Ce:YAG-Al<sub>2</sub>O<sub>3</sub> eutectics are promising materials for white LED application.

